High Power Laser Science and Engineering, (2024), Vol. 12, e52, 6 pages.
doi:10.1017/hpl.2024.34

HIGH POWER LASER SCIENCE AND ENGINEERING

RESEARCH ARTICLE

An electro-optic KLTN refractive index gradient deflector implemented in an actively *Q*-switched Tm:YLF laser

Salman Noach[1], Yechiel Bach[1], Mulkan Adgo[2], Yehudit Garcia[2], and Aharon J. Agranat[2]

[1] *Department of Electro-optics, Jerusalem College of Technology, Jerusalem, Israel*

[2] *Institute of Applied Physics, The Hebrew University of Jerusalem, Jerusalem, Israel*

(Received 19 February 2024; revised 9 May 2024; accepted 21 May 2024)

Abstract

A novel electro-optic deflector based on a quadratic electro-optical potassium lithium tantalate niobate (KLTN) crystal operating slightly above the ferroelectric phase transition is presented. The new deflection scheme was based on the electric field gradient generation along the vertical axis caused by the trapezoidal geometry of the crystal. A deflection angle of 6.5 mrad was attained for a low voltage of 680 V. The deflector was used as an electro-optic modulator for implementing active *Q*-switching in a thulium-doped yttrium lithium fluoride (Tm:YLF) laser (1880 nm). The laser was operated at three different repetition rates of 0.4, 0.5 and 0.7 kHz, and reached high energies per pulse up to 6.9 mJ.

Keywords: 2 μm lasers; electro-optic deflectors; electro-optic modulators; *Q*-switched lasers

1. Introduction

We report herein a new configuration for implementing active *Q*-switching in solid-state laser systems by deflecting the beam that traverses the laser resonator off its course during the accumulation of the population inversion. The deflection of the laser beam was realized by using an electro-optic (EO) potassium lithium tantalate niobate (KLTN) crystal in the shape of a trapezoidal prism. Applying an electrical pulse across the sides of the trapeze produces a refractive index gradient that deflects the beam off the optical axis of the resonator.

KLTN is a ferroelectric crystal with composition given by $K_{1-\beta}Li_{\beta}Ta_{1-\alpha}Nb_{\alpha}O_3$. Its phase transition temperature (T_c) is determined by the ratios [Nb]/[Ta] and [Li]/[K]. In the paraelectric phase, its EO effect is quadratic, and becomes exceptionally strong upon approaching T_c[1]. As opposed to its structural analog, potassium tantalate niobate (KTN), in close proximity to T_c, KLTN maintains its high optical quality and exhibits fast EO switching[2]. KLTN can be used as an EO medium in the wavelength range [0.4, 5.5 μm] through which it remains transparent.

In addition, by nature of the fact that at the paraelectric phase the EO effect is quadratic, photorefractive optical damage in the KLTN can be suppressed by operating the device with a bi-polar driving voltage. As such, this active *Q*-switch configuration enables one to exploit the fast EO effect in KLTN crystals irrespective of the polarization of the lasing beam, while avoiding the damaging effect of photons at visible wavelengths generated by the two-photon process in the laser crystal by the high-power pumping beam. This configuration is demonstrated effectively in a thulium-doped yttrium lithium fluoride (Tm:YLF) laser system that emits in the 2 μm spectral range (1880 nm), but the wide operable wavelength range of KLTN at the paraelectric phase enables its exploitation in other solid-state laser systems as well.

Lasers operating in the 2 μm region have many applications in a variety of fields, such as gas spectroscopy, medical micro-surgery, material processing, light detection and ranging (LIDAR), eye-safe free space communication and as a pumping source for mid-infrared (mid-IR) region lasers, for example, Cr:ZnSe and Cr:ZnS lasers[3]. Many applications require high-energy pulsed sources for obtaining a short exposure time, which results in mitigated thermal damage. This brings forwards the need for lasers that employ active *Q*-switching for producing high-energy narrow pulses.

Q-switched lasers operate by modulating the losses in the cavity. While the losses are enlarged, the stimulated emission is inhibited, allowing the population inversion to

Correspondence to: A. J. Agranat, Institute of Applied Physics, The Hebrew University of Jerusalem, Jerusalem 9190401, Israel. Email: agranat@savion.huji.ac.il; S. Noach, Department of Electro-optics, Jerusalem College of Technology, Jerusalem 9372115, Israel. Email: salman@jct.ac.il

accumulate. Once the losses are reduced, the high gain due to the high level of the population inversion causes the energy accumulated in the gain medium to be released in the form of a short and intense pulse[4].

As opposed to passive *Q*-switching where the pulses are emitted with fixed energy and slight jitter at the repetition rate, in active *Q*-switching the system operator can control the output energy, and the time when each pulse is generated. This is advantageous for numerous applications, including LIDAR systems, advanced imaging, precise material processing and laser micro-surgery. Active *Q*-switching can be achieved by employing either acousto-optic or EO modulators.

EO modulators are usually used as intensity modulators. In this implementation the EO crystal is used with a quarter wave plate to change the polarization of the laser beam. The beam traverses a polarizing cube with a perpendicular polarization and is deflected from the resonator. EO deflectors constitute a rare class of EO modulators. In these devices the laser beam is deflected through a refractive index gradient that is induced using the EO effect.

Implementing active *Q*-switching by beam deflection offers several advantages over alternative EO modulators. Firstly, it obviates the need for additional optical components such as a polarizing cube or a quarter wave plate. Secondly, its voltage requirement remains independent of the wavelength, enabling operation at longer wavelengths without adjustment. However, one drawback is its relatively small deflection angle.

In 2013, Huang *et al.*[5] presented a Nd:YVO_4 optical parametric oscillator (OPO) laser at 1550 nm with 8 μJ and 1 kHz using a deflector as a *Q*-switch modulator. In 1998, Conroy *et al.*[6] presented a potassium titanyl phosphate (KTP) OPO laser at 1064 nm with 4 μJ and 1–20 kHz using a deflector as a *Q*-switch modulator. In 2011, Miyazu *et al.*[7] presented a KTN deflector. This deflector utilized the EO effect gradient, caused by the field induced by the density gradient of trapped electrons implanted orthogonally to the optical axis, and the external field applied across the crystal. The combined effect of these two fields generated through the quadratic EO effect resulted in a refractive index gradient that caused the traversing beam to deflect.

We present herein a novel and different deflection scheme, based on the trapezoidal shape of the KLTN crystal. The KLTN crystal operating at the paraelectric phase manifests a quadratic EO effect that, upon approaching the ferroelectric phase transition, becomes remarkably large, exhibiting an electrically induced change in the refractive index of approximately 0.015 while maintaining high optical quality[8].

As described above, deflection is obtained by using a trapezoidal shape crystal, in which the voltage applied to electrodes deposited on the slanted sides of the trapeze generates a gradient in the field induced in the crystal across the wave-front of the propagating beam. Thus, when the voltage across the crystal is activated, the field across the propagating beam varies, which through the EO effect produces a refractive index gradient that causes the beam to deflect. A deflection of 6.5 mrad was achieved for a low operating voltage of 680 V.

It should be noted that in our previous paper in which we described an active *Q*-switching scheme based on polarization modulation, we also used a trapezoidal crystal[9,10]. However, in that method, the trapezoid KLTN served as an active quarter wave plate switch, exploiting the variation in the emission cross-section between the two polarizations of the Tm:YLF and thulium-doped yttrium aluminum perovskite (Tm:YAP) crystals. Its geometrical shape was not a limited constraint of the method or crucial to its operations. The trapezoid shape there was used for damping raised acoustic noises for improving the modulator performance. The modulation of the laser was done by forcing a polarization in which the gain in the cavity is high or low depending on the value of the polarization cross-section. The main disadvantage of the polarization modulation method is that it is restricted only to limited types of anisotropic gain crystals, where there is a significant difference in the cross-section values between the two polarizations. In contrast, in the method presented herein, the KLTN crystal functions as a classic *Q*-switching device, producing controlled losses in the resonator. The KLTN trapezoidal geometric shape, and its cut, are obligatory to obtain a gradient in the refractive index that causes the deflection effect. This method is not limited to anisotropic crystals and can be applied in isotropic crystals as well. A proof of concept for producing deflection in a trapezoidal KLTN crystal operating at the 2 μm spectral range, and its employment for implementing *Q*-switching in a Tm:YLF laser, are presented here for the first time. As described henceforth, the laser was characterized at three different repetition rates of 0.4, 0.5 and 0.7 kHz, and high energies per pulse up to 6.9 mJ were achieved.

2. Experimental setup and results

The deflector was a KLTN crystal that was grown by the authors using the top seeded solution growth method[11].

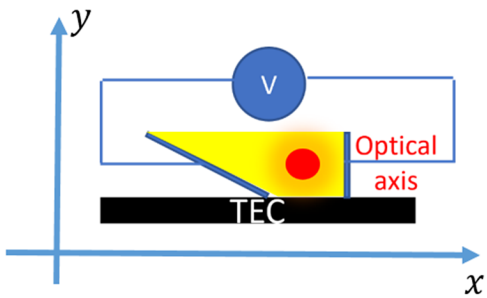

Figure 1. The deflector trapezoid cross-section.

https://doi.org/10.1017/hpl.2024.34 Published online by Cambridge University Press

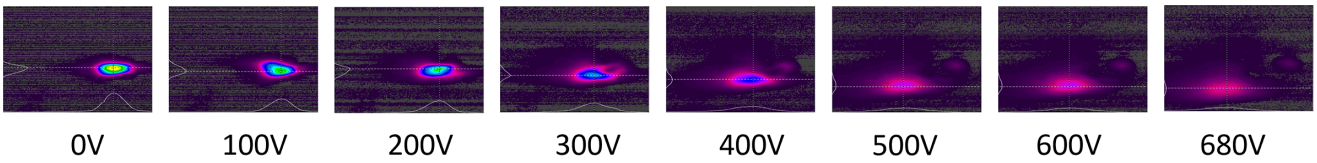

Figure 2. Beam deflection pictures at different voltages.

The KLTN crystal was 9 mm long, with a trapezoidal cross-section that is 2 mm high and with bases of 2 and 6 mm. The KLTN cross-section is shown in Figure 1. Its facets that were perpendicular to the optical axis of the resonator were coated with anti-reflective coating for $\lambda = 1880$ nm. Aluminum electrodes were deposited on the opposite-side facets of the trapezoidal prism. The KLTN crystal was placed on a thermal electrical cooler and its temperature was set to 20°C, which is 6°C above the KLTN crystal phase transition temperature, in order to enlarge the effect of the applied voltage[1]. The deflection angle as derived from the Eikonal equation is given by the following:

$$\theta_{\text{def}} = \frac{\mathrm{d}n}{\mathrm{d}y} L, \tag{1}$$

where L is the crystal length and $\frac{\mathrm{d}n}{\mathrm{d}y}$ is the induced refractive index gradient, which is caused by the variation of the EO effect. The expression for the EO effect in KLTN at the paraelectric phase is as follows:

$$\Delta n(E) = -\frac{1}{2} n^3 g_{\text{eff}} \varepsilon^2 E(y)^2 = -\frac{1}{2} n^3 g_{\text{eff}} \varepsilon^2 \left(\frac{V}{d(y)} \right)^2, \tag{2}$$

where $\Delta n(E)$ is the electrically induced change in the refractive index, n is the refractive index of the KLTN at the paraelectric phase, g_{eff} is the effective (quadratic) EO coefficient, ε is the dielectric constant, $E(y)$ is the applied electric field (which varies along the vertical axis), V is the applied voltage and d is the varying distance between the electrodes.

The variation of the EO effect is inversely dependent at the squared distance between the electrodes, which varies linearly along the vertical axis. Thus, the expression for the deflection angle is given by the following:

$$\theta_{\text{def}} = -\frac{1}{2} n^3 g_{\text{eff}} V^2 \frac{\mathrm{d}}{\mathrm{d}y} \left(\frac{\varepsilon^2}{d^2} \right) L, \tag{3}$$

where θ_{def} is the deflection angle of the propagating beam. It is also assumed that the dielectric constant in Equation (3) varies across the vertical coordinate of the crystal ($\varepsilon = \varepsilon(y)$) due to the temperature gradient across the crystal. The KLTN crystal was placed on its short base in order to align the thermal gradient with the direction of the electric field gradient.

2.1. *Off-cavity characterization*

Prior to testing the active Q-switching scheme, the deflection of the KLTN crystal was measured outside the Tm:YLF laser cavity. The input beam was collimated to a beam diameter of 1 mm. A pyroelectric camera (Pyrocam III-HR, Spiricon) was placed 725 mm after the KLTN crystal. The deflection angle was measured by examining the camera images.

The camera pictures at different voltages are shown in Figure 2. Maximal angles of deflection of 6.5 mrad at the vertical axis and of 2.9 mrad at the horizontal axis were observed for a voltage of 680 V, as shown in Figure 3, and the curve profiles are parabolic as expected, since the deflection is dependent on the square of the applied voltage, as presented in Equation (3).

2.2. *On-cavity characterization*

Following the characterization measurements of the KLTN gradient deflector, a Tm:YLF laser system was built, in which the KLTN gradient deflector served as the Q-switching apparatus. The laser system is shown in Figure 4. The Tm:YLF laser was pumped by a 30 W fiber coupled diode laser operating at 793 nm, which was collimated and focused to a spot diameter of 440 μm on the gain medium, using a pair of plano convex lenses with focal lengths of 40 and 100 mm, respectively. The Tm:YLF cavity included a plano input mirror with high transmission for the pumping wavelength (793 nm) and high reflectance for the Tm:YLF wavelength (1880 nm). The Tm:YLF crystal (3% atomic fraction) was 15 mm long with a cross-section of 3 mm × 3 mm. The Tm:YLF crystal was oriented so

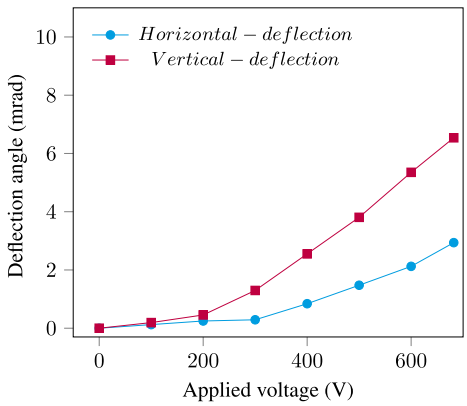

Figure 3. Deflection angle versus the applied voltage.

https://doi.org/10.1017/hpl.2024.34 Published online by Cambridge University Press

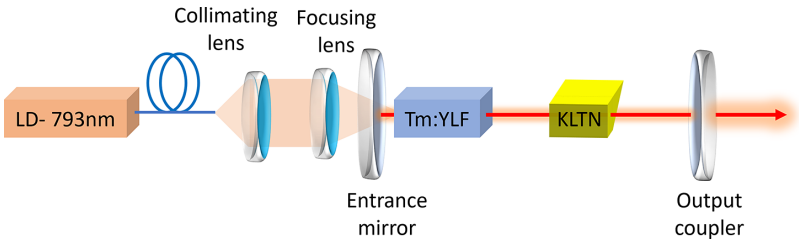

Figure 4. The system scheme of the actively Q-switched Tm:YLF laser based on an EO KLTN deflector.

that its emitted beam polarization was parallel to the applied voltage direction, since the EO coefficient is larger in this way[8]. The output coupler had a radius of curvature of 200 mm and was 55% partially reflective for the Tm:YLF wavelength (1880 nm).

As can be seen in Figure 4, the laser was designed so that the undeflected beam that traverses the KLTN crystal is co-aligned with the cavity axis, whereas activating the field across the KLTN crystal caused the transmitted beam to deflect sideways and distort, as presented in Figure 2. Thus, applying the field across the KLTN crystal induces losses in the cavity that prevent lasing, so that the population inversion is allowed to accumulate.

The KLTN crystal was positioned as far as possible from the output coupler's focal point (and, therefore, very close to the output coupler) in order to maximize the influence of the applied voltage on the induced losses in the cavity (taking into account that the minimum distance between the output coupler and the KLTN crystal was limited due to the relatively large beam diameter near the output coupler, and the KLTN dimensions). The effect of the losses caused by the applied voltage on the laser performance was measured when the laser was operated in the continuous-wave (CW) mode. The output power was measured, after filtering the residual pump power, using a power meter (Ophir, L50(150)A-35).

The Tm:YLF laser emitted 4.1 W for 25 W of pumping power while the applied voltage was off. While the applied voltage was 680 V the Tm:YLF laser emitted 2 W, which is about 50% of the full output power. The influence of the applied voltage on the laser output power is presented in Figure 5. It is seen in Figure 5 that the influence of low voltages is minor, which was expected since the deflection was small at low voltages, as presented in Figure 3.

The laser was then operated in a pulsed mode. It should be noted that the Tm:YLF crystal, when pumped at high power, generates blue photons due to the upconversion process[12]. These generate a photorefractive space-charge in the KLTN crystal causing optical damage, which mitigates the laser operation. This hurdle was overcome by operating the KLTN deflector with a bi-polar driving voltage (with a rise and fall time of approximately 30 ns). As shown in Ref. [13], due to the fact that the EO effect in the KLTN crystal at the paraelectric phase is quadratic, this does not affect the propagating beam, but prevents the photorefractive space-charge

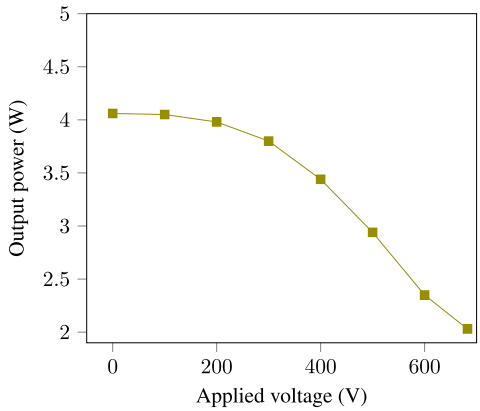

Figure 5. Influence of the applied voltage on the laser output power.

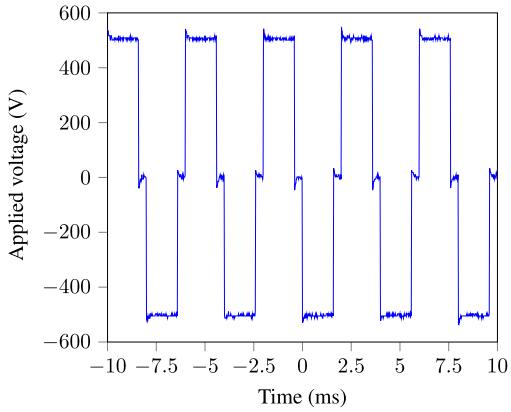

Figure 6. The bi-polar modulated voltage profile versus time, at a repetition rate of 0.5 kHz.

from being accumulated, so that optical damage is avoided. The time dependence of the modulating voltage is shown in Figure 6. The energy per pulse under this bi-polar modulated voltage was then measured versus the input pump power.

The pulse energy was measured with an energy meter (Ophir, PE50-C). Pulse temporal characterization was performed using an extended InGaAs fast photodetector with 28 ps rise-time (EOT, ET-5000, 12.5 GHz) and a 100 MHz oscilloscope (Agilent, DSO5012A).

In the pulsed mode, a considerably low voltage of 500 V was applied on the KLTN crystal. The laser was operated at three different repetition rates of 0.4, 0.5 and 0.7 kHz. EO crystals are commonly limited by acoustic waves that disturb the optical response at high repetition[14]. Such acoustic

https://doi.org/10.1017/hpl.2024.34 Published online by Cambridge University Press

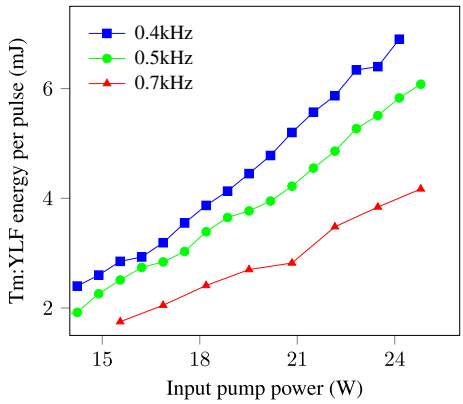

Figure 7. Tm:YLF energy per pulse at 0.4, 0.5 and 0.7 kHz.

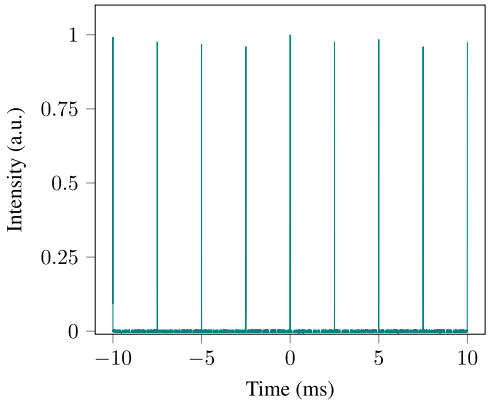

Figure 9. Tm:YLF pulse train at 0.4 kHz.

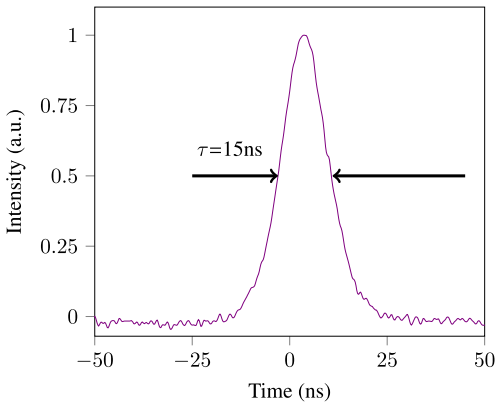

Figure 8. Tm:YLF laser pulse temporal profile of 15 ns.

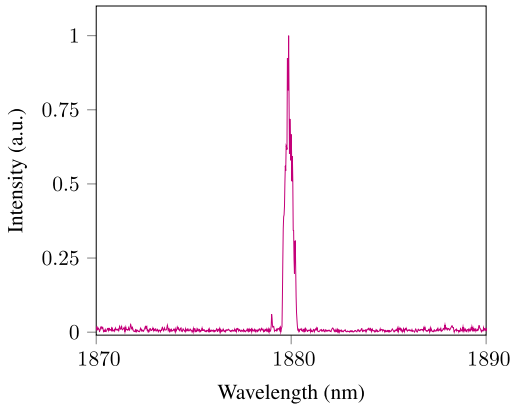

Figure 10. Tm:YLF laser spectrum acquired by a pulsed laser spectrum analyzer (Bristol, 772B).

waves occur at the KLTN crystal as well[2,9,10,15], which could be the reason why the laser did not exceed the repetition rate of 0.7 kHz. At 0.4 kHz the laser generated pulses with energy of 6.9 mJ per pulse corresponding to a slope efficiency of 18.7%, and optical-to-optical conversion of 11.4%. At 0.5 kHz the laser generated pulses with energy of 6.1 mJ per pulse corresponding to a slope efficiency of 18.9%, and optical-to-optical conversion of 12.2%. At 0.7 kHz the laser generated pulses with energy of 4.2 mJ per pulse corresponding to a slope efficiency of 18.4%, and optical-to-optical conversion of 11.8%. The energy per pulse is presented in Figure 7. The pulse temporal profile of a representative 15 ns duration is presented in Figure 8. The laser pulse stability can be seen at the pulse train measurement taken at 0.4 kHz, and is shown in Figure 9. The laser emitted at the wavelength of 1880 nm with a spectral bandwidth of 0.4 nm is presented in Figure 10.

3. Conclusion

In conclusion, a novel EO deflector based on a KLTN crystal, which was cut in the shape of a trapezoidal prism, performed as an EO index gradient deflector. Off cavity, the deflector produced a deflection of 6.5 mrad. With the deflector positioned inside the Tm:YLF cavity, the laser was operated at three different repetition rates of 0.4, 0.5 and 0.7 kHz, and obtained 6.9, 6.1 and 4.2 mJ energies per pulse, respectively. This is the first demonstration of a KLTN crystal as an EO deflector for implementing active *Q*-switching. This constitutes a first demonstration of performing active *Q*-switching using an EO gradient deflector implemented by a KLTN crystal at the paraelectric phase. This configuration for performing active *Q*-switching is independent of the beam polarization and the gain medium crystalline structure, and as such is inherently more efficient than other EO active *Q*-switching configurations, while exploiting the inherent speed of EO switching.

Acknowledgement

This project was supported by the Israel Ministry of Science, Technology and Space, Grant No. 88428.

References

1. G. Hirshfeld, Y. Vidal, Y. Garcia, G. Perepelitsa, A. Karsenty, Y. Kabessa, and A. J. Agranat, Results Phys. **23**, 104059 (2021).
2. Y. Vidal, S. Noach, and A. J. Agranat, Proc. SPIE **11281**, 112811T (2020).

https://doi.org/10.1017/hpl.2024.34 Published online by Cambridge University Press

3. K. Scholle, S. Lamrini, P. Koopmann, and P. Fuhrberg, in *Frontiers in Guided Wave Optics and Optoelectronics* (IntechOpen, 2010), Chap. 22.
4. O. Svelto and D. C. Hanna, *Principles of Lasers* (Springer, 2010).
5. J. F. Huang, W. K. Chang, H. P. Chung, S. S. Huang, J. W. Chang, and Y. H. Chen, Opt. Express **21**, 30370 (2013).
6. R. S. Conroy, C. F. Rae, G. J. Friel, M. H. Dunn, B. D. Sinclair, and J. M. Ley, Opt. Lett. **23**, 1348 (1998).
7. J. Miyazu, T. Imai, S. Toyoda, M. Sasaura, S. Yagi, K. Kato, Y. Sasaki, and K. Fujiura, Appl. Phys. Express **4**, 111501 (2011).
8. A. Gumennik, Y. Kurzweil-Segev, and A. J. Agranat, Opt. Mater. Express **1**, 332 (2011).
9. S. Noach, R. Nahear, Y. Vidal, Y. Garcia, and A. J. Agranat, Opti. Lett. **46**, 1971 (2021).
10. R. Nahear, Y. Bach and S. Noach, Opt. Laser Technol. **146**, 107548 (2022).
11. R. Hofmeister, A. Yariv, and A. Agranat, J. Crystal Growth **131**, 486 (1993).
12. X. X. Zhang, P. Hong, M. Bass, and B. H. T. Chai, Phys. Rev. B **51**, 9298 (1995).
13. Y. Kabessa, A. Yativ, and A. J. Agranat, Opt. Express **23**, 4348 (2015).
14. M. Roth, M. Tseitlin, and N. Angert, Glass Phys. Chem. **31**, 86 (2005).
15. R. Nahear, Y. Vidal, S. Noach, and A. J. Agranat, Proc. SPIE **11259**, 112590X (2020).

https://doi.org/10.1017/hpl.2024.34 Published online by Cambridge University Press